

## Water-preserved coal mining in water-shortage mining areas: a case study in the Yonglong mining area of China

Xiuchang Shi<sup>a,b,\*</sup> and Guangluo Lyu<sup>b,c</sup>

<sup>a</sup> School of Engineering Management and Real Estate, Henan University of Economics and Law, Zhengzhou 450046, China

<sup>b</sup> Key Laboratory of Coal Resources Exploration and Comprehensive Utilization, Ministry of Land and Resources, Xi'an 710021, China

<sup>c</sup> Shaanxi 186 Coalfield Geological Co Ltd, Xi'an 710075, China

\*Corresponding author. E-mail: sxccumb@126.com

### ABSTRACT

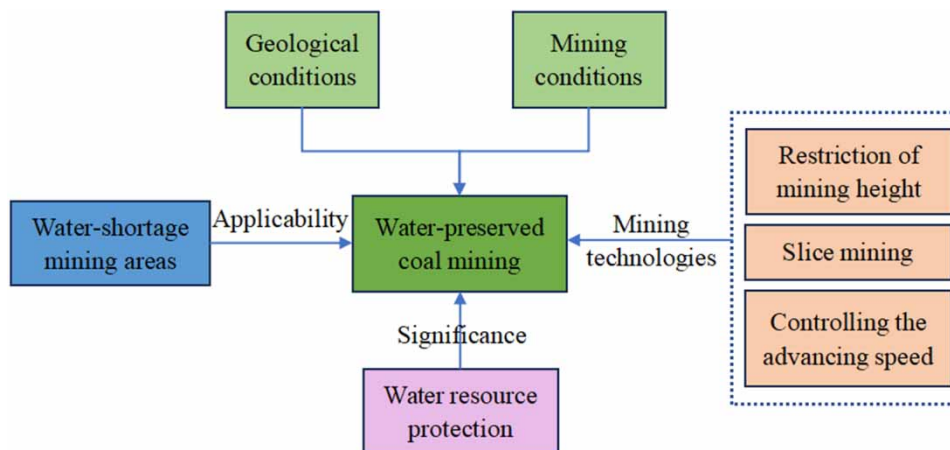
Water-preserved coal mining (WPCM) in water-shortage mining areas is an important aspect of water resources management. This paper aimed at the protection of Cretaceous groundwater resources during the high-intensity mining in the Yonglong mining area, China, and carried out basic theory and practical application of WPCM. The hydrogeological structure and engineering geological characteristics were investigated on-site. On-site detection and numerical simulation were used to study the dynamic evolution laws of overburden failure and water-conducting fractured zone (WCFZ), and the seepage laws of mining-induced overburden were analyzed by the rock triaxial seepage test. The results showed that it was feasible to carry out WPCM in the Yonglong mining area. From the view of reducing the height of WCFZ and preventing water hazards, the technical measures for WPCM were proposed. The research results can provide a theoretical basis and technical approach for WPCM in the water-shortage mining areas.

**Key words:** hydrogeological structure, mining technical measures, overburden failure, water-conducting fractured zone, water-preserved mining

### HIGHLIGHTS

- The feasibility of water-preserved coal mining was analyzed.
- Overburden failure and seepage laws induced by coal mining were studied.
- Water-preserved coal mining technologies were proposed.

### GRAPHICAL ABSTRACT



### ABBREVIATIONS

WPCM water-preserved coal mining

WCFZ water-conducting fractured zone

This is an Open Access article distributed under the terms of the Creative Commons Attribution Licence (CC BY 4.0), which permits copying, adaptation and redistribution, provided the original work is properly cited (<http://creativecommons.org/licenses/by/4.0/>).

## 1. INTRODUCTION

Coal provides an important energy guarantee for the global economic development, but its mining also causes a lot of damage and waste to the precious groundwater resources in the mining area (Zhang 2005; Booth 2006; Zhang *et al.* 2011; Sun *et al.* 2016). During coal mining, water resources will be consumed and destroyed. According to statistics, about 2 tons of mine water will be produced for each ton of coal mined. Coal mine surface subsidence has a serious impact on surface water runoff and surface environment, and mine water discharge will also pollute water resources (Booth & Bertsch 1999; Liu & Elsworth 1999; Guo *et al.* 2019; Qiu *et al.* 2019). Most of the large coal bases in the world are located in areas where the contradiction between supply and demand of water resources is relatively prominent. For example, among the 96 state-owned key mining areas in China, water-shortage mining areas account for 71% (Cao 2017). The shortage of water resources seriously restricts the coal consumption and mining (Shi & Zhang 2021). Therefore, how to maximize the protection and utilization of water resources while coal mining is an inevitable requirement for sustainable development strategy.

Since the 1970s, the contradiction between the expanding scale of global coal production and the water environment has become increasingly acute, attracting the attention of governments and scholars (Booth 1986; Zipper *et al.* 1997). For example, in the 1970s, the United States has paid attention to the contradiction between coal mining and water consumption in the Yellowstone River watershed, and began to study the competition of water resources among industry, agriculture and other industries (Thomas & Anderson 1976). The Tongue River Basin in Montana entered the period of large-scale coal mining in the 1980s, and also began to study the phenomena of riverbed drainage, water quality deterioration and aquatic ecosystem damage induced by mining (Hickcox 1980). Some European countries mainly focus on the treatment mechanism and technology of mine water, the impact of abandoned mine water discharge on the environment and have conducted legislative and technical research on the protection of mine water resources (Gombert *et al.* 2018). The geological and hydrogeological conditions of mines in Australia, India, South Africa and other countries are relatively simple, and more attention is paid to the utilization of mine water and the treatment and utilization of open pit ponding lakes (Tiwari *et al.* 2016). In the 1990s, coal mining in the early stage of the development of Yushenfu mining area in China caused water environment problems such as the decline of phreatic water level and the drying up of springs. Some scholars initially proposed the thinking and method of water-preserved coal mining (WPCM), and thought that coal mining, water conservation, and ecological environment protection should be unified planning as a system engineering (Fan & Ma 2018; Fan *et al.* 2019a; Yu & Ma 2019). After decades of development, countries around the world have made great achievements in theoretical research and engineering practice of water resources and ecological environment protection in mining areas.

Aiming at the protection of groundwater resources during the high-intensity mining of Yonglong mining area of Huanglong Jurassic coalfield in western China, this paper analyzed the hydrogeological structure and engineering geological characteristics, studied the overburden failure and seepage laws during the mining of extra-thick coal seam, and put forward some protective mining technologies suitable for the study area. The research results are of great significance to the protection of water resources, ecological environment and the realization of sustainable development of water-shortage mining areas.

## 2. GEOLOGICAL SETTING

### 2.1. Hydrogeological structure

Yonglong mining area is located in the west of Huanglong Coal Base in Shaanxi Province, China, and belongs to the Mesozoic confined water in Ordos Basin. The water-bearing bedrock strata are composed of clastic rocks of various grain sizes in the Lower Cretaceous, Jurassic and Triassic. The groundwater is mainly sandstone confined fissure water, followed by loose layer phreatic water. The sandstone aquifer is mainly Cretaceous pore-fissure aquifer and Jurassic–Triassic fissure aquifer. It is divided into two types of water storage structures: Cretaceous confined water syncline and Jurassic–Triassic confined water monocline. The Luohe Formation of the lower Cretaceous system is sporadically exposed in the surface valleys of the study area, and its upper Neogene and Quaternary systems are widely covered.

According to the hydrogeological data during the exploration and mine construction of Yonglong mining area, the lithology, structure and water abundance of the strata are comprehensively analyzed. Then the aquifers in the

overlying strata of the main mining No. 3 coal seam are divided into seven layers, and the aquicludes are divided into two layers, as shown in Table 1.

**Table 1** | Division of aquifers and aquicludes in the overlying strata

Stratum code	Numbering	Name of aquifers and aquicludes	Thickness (m)	Permeability coefficient ( $\text{m} \cdot \text{s}^{-1} \cdot \text{m}^{-1}$ )
$Q_4$	I	Quaternary Holocene alluvial-proluvial pore phreatic aquifer	0–8	–
$Q_{2+3}$	II	Quaternary Middle-Upper Pleistocene loess pore-fissure phreatic aquifer	5–150	–
$N_2$	III	Neogene clay aquiclude	60	–
$N_1$	IV	Neogene sandy gravel aquifer	3–5	–
$K_{1l}$	V	Lower Cretaceous Luohe Formation sandstone pore-fracture aquifer	103.1–329.3	0.00899–0.1908
$K_{1y}$	VI	Lower Cretaceous Yijun Formation glutenite fracture aquifer	20.5–60.9	0.0088
$J_{2a}$	VII	Middle Jurassic Anding Formation mudstone aquiclude	68.56–196.4	0–0.000076
$J_{2z}$	VIII	Middle Jurassic Zhiluo Formation sandstone fracture aquifer	10–50	0.004578
$J_{2y}$	IX	Middle Jurassic Yan'an Formation coal seam and its roof sandstone aquifer	5–60	0.003431

It can be seen from Table 1 that the Anding Formation mudstone aquiclude in the Middle Jurassic System has large thickness, stable horizon, good continuity and good water resistance. It is a stable aquiclude between the coal measures and the overlying Cretaceous aquifer, and is the water-resisting key stratum in water-preserved mining, belonging to the high-level aquiclude structure (Miao *et al.* 2009). In the process of coal seam mining, the sandstone aquifer in the Middle Jurassic Zhiluo Formation, the Yan'an Formation coal seam and its roof sandstone aquifer are the direct water-filled aquifers. Because of their deep burial depth, underdeveloped fractures, poor recharge conditions, and weak water abundance, mine water filling is easy to drain, which has little effect on coal seam mining. Although the lower Cretaceous sandstone aquifer is an indirect water-filled aquifer of coal seam roof, it is thick, widely distributed, and has good water yield, and is connected with the regional aquifer with strong water abundance. Many water inrush accidents have occurred during the construction and production of the mine, resulting in the shutdown of the mine and the loss of groundwater resources. Therefore, the groundwater in the Cretaceous sandstone aquifer is not only an important regional water supply source, but also the main source of mine water inrush. To conclude, it is urgent to carry out water hazard prevention and groundwater resources protection.

## 2.2. Engineering geological characteristics

The thickness of the overlying strata between the No. 3 coal seam roof and the Cretaceous sandstone aquifer is 125.43–277.80 m, with an average of 185.80 m, which is mainly composed of three sets of rock groups: Anding Formation, Zhiluo Formation and Yan'an Formation. The lithology combination of each rock group is mainly medium sandstone-coarse sandstone, siltstone -fine sandstone, and mudstone-sandy mudstone. Mudstone, sandy mudstone and siltstone of Anding Formation, Zhiluo Formation and Yan'an Formation are relatively thick, with an average cumulative thickness of 102.08 m. The test results of mudstone disintegration and expansion in the study area are shown in Table 2. From Table 2, it can be seen that the mudstone and sandy mudstone in the overlying strata have the characteristics of easy disintegration and good expansibility when meeting with water, which will lead to the closure of mining-induced fractures and reduce the development height of water-conducting fractured zone (WCFZ), thus restoring the ability to block the runoff of Cretaceous aquifer to mine goaf. To conclude, this lithology combination of overlying strata plays a positive role in water-preserved mining and mine water disaster prevention, indicating that the study area has the basic geological conditions to realize water-preserved mining.

**Table 2** | Disintegration and expansion test data

Stratum lithologic	Free swelling rate $\delta_{ef}$ (%)	Expansion force $p_e$ (MPa)	Loaded expansion rate at 0.01 MPa $\delta_p$ (%)	Disintegration resistance index $I_{d2}$ (%)
Anding formation sandy mudstone	27.92	17.8	31.85	4.47
Anding formation mudstone	29.55	36.9	33.2	3.01
Zhiluo formation sandy mudstone	23.61	13.6	25.79	7.65
Yan'an formation sandy mudstone	25.33	16.3	28.15	7.37

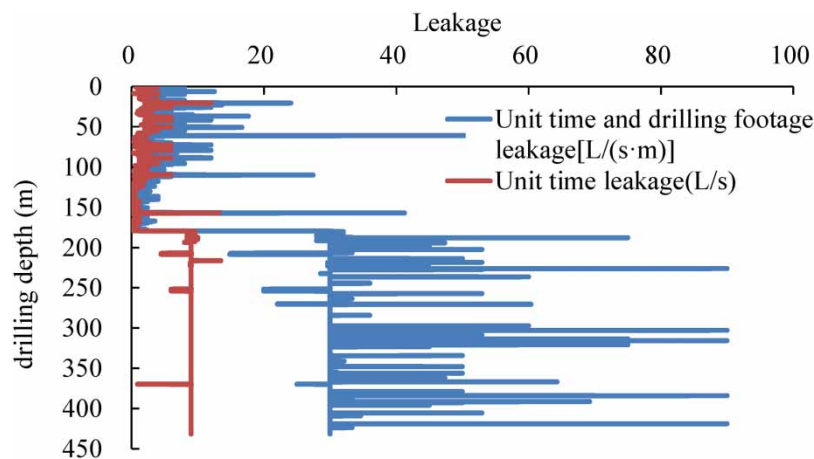
### 3. MINING-INDUCED OVERBURDEN FAILURE AND SEEPAGE LAWS

#### 3.1. Mining-induced overburden failure laws

##### 3.1.1. Field detection of WCFZ height

Determining the WCFZ height is the basis for implementing the WPCM. In this paper, the WCFZ height was determined by observing the drilling fluid leakage and the water level change in the borehole. G1 borehole was a post-mining drilling fluid leakage detection hole and was also used for post-mining peeping detection. The G1 borehole was located above the No. 20301 working face of Cuimu coal mine. The mining thickness of the working face was 12 m, and the vertical depth from the coal seam floor to the orifice was 553.22 m.

When the drilling depth was 179.29 m, the flushing fluid completely leaked, and the buried depth of water level in the borehole decreased from 47.1 to 79.6 m. When the drilling depth was 302.75 m, the buried depth of water level suddenly dropped from 86.2 to 124.5 m, as shown in Figures 1 and 2. In the subsequent drilling, the water level in the borehole continued to drop significantly. Before drilling to the borehole depth of 302.75 m, there was sand sedimentation in the borehole after each lifting. In the subsequent construction, the sand sedimentation gradually disappeared, and the boring crown dropped and stuck for many times, resulting in two drill pipe accidents in the borehole.

**Figure 1** | Variation curve of flushing fluid leakage in the G1 borehole.

Based on the comprehensive analysis of the changes of flushing fluid leakage, water level and abnormal phenomena during drilling rig construction, the borehole depth of 302.75 m was defined as the top boundary of WCFZ, which was 238.47 m away from the No. 3 coal seam.

The calculation formula for the height of WCFZ is as follows:

$$H_f = H_s - M - h + W \quad (1)$$

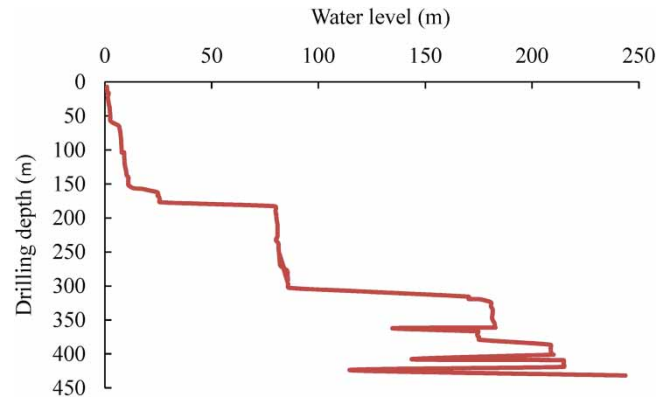


**Figure 2** | Variation curve of groundwater level in the G1 borehole.

where  $H_f$  is the WCFZ height;  $H_s$  is the vertical depth of No. 3 coal seam floor from the porthole;  $M$  is the mining height;  $h$  is the vertical depth between the top of WCFZ and porthole;  $W$  is the compression value of fractured zone strata during drilling observation ( $W = 0.2$  m here).

Through calculation, the WCFZ height is 238.67 m, and the ratio of WCFZ to mining height is 19.89.

### 3.1.2. Numerical simulation of the height of WCFZ

Based on the stratum structure of No. 21301 working face in Cuimu coal mine, a three-dimensional numerical model was established by using FLAC3D 6.0 software, with dimensions of 900 m long, 300 m wide and 302 m high. The design mining length of the working face was 700 m along the strike direction, 200 m along the sloping direction, and the mining height was 12 m. The boundary conditions of the numerical model were as follows: the horizontal displacement was limited on the side of the model, the vertical displacement and horizontal displacement were limited on the bottom, and the vertical load (about 7 MPa) was applied on the top to simulate the self-weight stress of the overlying rock. Elastic constitutional model was used for the initial stress simulation and the Mohr–Coulomb yielding criterion was used in the excavation simulation. The rocks are elastic–plastic media in terms of the laboratory results and the physical–mechanical parameters used in FLAC3D simulation are shown in Table 3.

**Table 3** | Stratum structure and physical–mechanical parameters of rocks

Stratum	Lithology	Thickness (m)	Density (Kg/m <sup>3</sup> )	Bulk modulus (GPa)	Shear modulus/ (GPa)	tensile strength (MPa)	Cohesion (MPa)	angle of internal friction (°)
Luohe Formation	Medium sandstone	45	2,750	23.83	16.78	4.0	4.47	39
Yijun Formation	Glutenite	25	2,680	20.98	12.81	3.7	3.68	37
Anding Formation	Siltstone-mudstone interbedding	100	2,510	9.02	4.61	1.5	2.18	33
Zhiluo Formation	Fine sandstone- siltstone interbedding	65	2,630	12.36	7.59	1.8	2.53	34
Yan'an Formation	Sandy mudstone	35	2,560	10.58	6.02	1.9	1.32	36
	No. 3 coal	12	2,380	7.35	4.05	1.2	1.50	35
	Siltstone	20	2,520	9.58	5.12	2.0	2.23	36

The relationship between the development height of WCFZ and the mining length calculated by numerical simulation is shown in Figures 3 and 4. When the working face advanced 100 m, the WCFZ height was 38 m, penetrating the Yan'an Formation and entering the Zhiluo Formation. When the working face advanced 300 m, the WCFZ height was 112 m, penetrating the Zhiluo Formation and entering the Anding Formation. When the working face advanced 600 m, the fully mining was basically achieved. The maximum height of WCFZ was 245 m, and it has penetrated into the Luohe Formation strata, that is, the water leakage channel between the Luohe Formation aquifer and the goaf was formed. Since then, with the increase of the length of

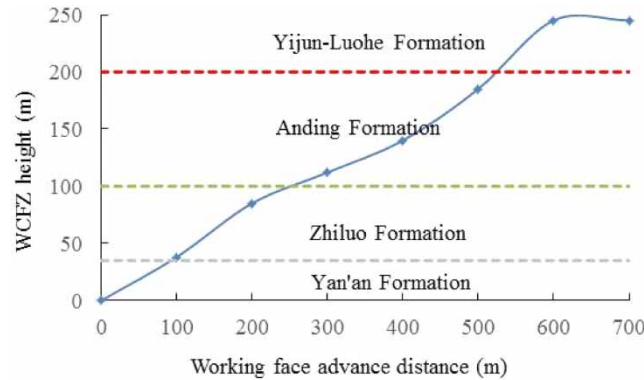


**Figure 3** | Relationship between the height of WCFZ and the advancing distance of working face.

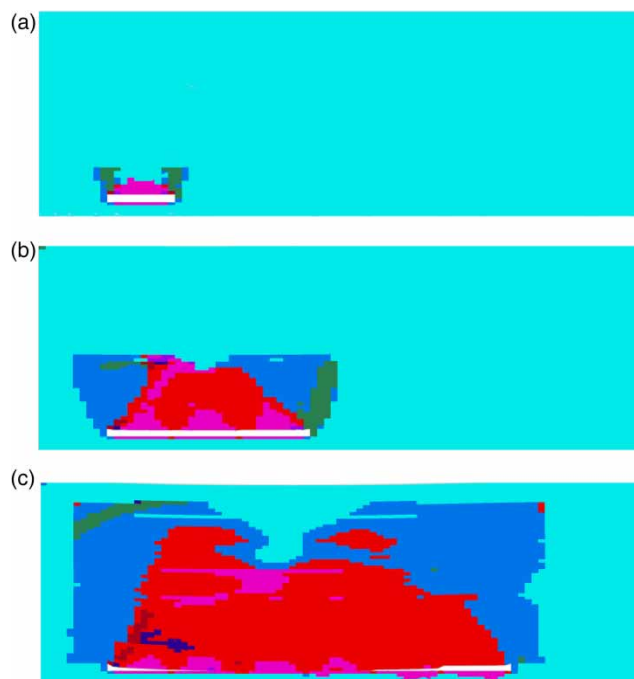


**Figure 4** | Plastic failure zone of overlying strata during coal seam mining: (a) advancing distance of 100 m, (b) advancing distance of 300 m, and (c) advancing distance of 600 m.

coal seam mining, the range of WCFZ was expanded, but its height remained basically unchanged. The distribution pattern of the plastic zone of mining-induced overburden failure was saddle-shaped. The rock mass in the middle of the goaf was mainly tensile failure, and the rock mass on both sides was mainly shear failure.

### 3.1.3. Spatial relationship between WCFZ and cretaceous aquifer

The measured data of the WCFZ height under the condition of fully mechanized top-coal caving mining in the extra-thick coal seam in Yonglong mining area were collected, as shown in Table 4.

According to the measured values of the development height of WCFZ, the average ratio of WCFZ to mining height in Yonglong mining area is determined to be 20.67, and the maximum height of WCFZ in different boreholes under the full-thickness mining conditions of the No. 3 coal seam in Cuimu coal mine is estimated using this ratio, as shown in Table 5.

It can be seen from Table 6 that when the mining height is greater than 9 m, the development height of WCFZ will generally penetrate the Cretaceous aquifer, leading to serious leakage of groundwater resources. However, when the mining height is less than 9 m, the development height of WCFZ will not penetrate the Cretaceous

**Table 4** | Measured values of the height of WCFZ in Yonglong mining area

Coal mine	Working face	Mining height (m)	WCFZ height (m)	Ratio of WCFZ to mining height
Cuimu	21301	12	238.7	19.9
Cuimu	21303	8.2	190.5	23.2
Cuimu	21305	10.86	230.9	21.3
Hujiahe	401110	12	252.0	21.0
Hujiahe	401106	13	225	17.3
Hujiahe	401101	10	225.4	22.3
Dafoshi	40106	11.22	192.1	17.1
Tingnan	206	7.5	140.2	18.7
Zhaoxian	1305	11.5	256.8	22.3
Zhaoxian	1307	11	198.8	18.1
Yuanzhigou	1012001	10.7	251.9	23.5
Guojiahe	1302	9	209.8	23.3

**Table 5** | Prediction of development height of WCFZ

Borehole	Thickness of No. 3 coal (m)	Distance from No. 3 coal to the bottom boundary of Cretaceous aquifer (m)	Estimated height of WCFZ (m)	Whether the WCFZ extends to the Cretaceous aquifer
G5-2	21.4	247.60	442.34	Yes (penetrates the aquifer by 194.74 m)
G5-3	15.4	211.70	318.32	Yes (penetrates the aquifer by 106.62 m)
G6-1	5.3	192.76	109.55	No (83.21 m away from the aquifer)
G6-4	20.1	273.71	415.47	Yes (penetrates the aquifer by 141.76 m)
G6-5	10.4	210.17	214.97	Yes (penetrates the aquifer by 4.8 m)
G6-6	5.6	210.33	115.75	No (94.58 m away from the aquifer)
G7-2	15.7	258.05	324.52	Yes (penetrates the aquifer by 66.47 m)
G8-3	15.8	235.02	326.59	Yes (penetrates the aquifer by 91.57 m)
G14-1	19.7	190.79	407.20	Yes (penetrates the aquifer by 216.41 m)
G14-2	10.4	189.39	214.97	Yes (penetrates the aquifer by 25.58 m)
G15-2	8.9	208.15	183.96	No (24.19 m away from the aquifer)
G15-3	10.6	218.44	219.10	Yes (penetrates the aquifer by 0.66 m)
G15-4	19.6	257.86	405.13	Yes (penetrates the aquifer by 147.27 m)
G15-5	14.4	225.45	297.65	Yes (penetrates the aquifer by 72.20 m)
G16-1	12.0	216.93	248.04	Yes (penetrates the aquifer by 31.11 m)
G16-3	15.9	263.79	328.65	Yes (penetrates the aquifer by 64.86 m)
G16-4	17.6	257.10	363.79	Yes (penetrates the aquifer by 106.69 m)
G16-5	11.2	249.63	231.50	No (18.13 m away from the aquifer)
G16-7	12.4	233.84	256.31	Yes (penetrates the aquifer by 22.47 m)
G17-2	13.9	238.78	287.31	Yes (penetrates the aquifer by 48.53 m)

aquifer. According to the hydrogeological background of the study area, the hydrogeological structure can be divided into high-level aquiclude structure, and the aquiclude is the mudstone of Anding Formation. After the mining of No. 3 coal seam, the sandstone fracture aquifer of Zhiluo Formation and the sandstone aquifer of Yan 'an Formation will be destroyed. Due to the existence of natural high-level aquiclude (Anding Formation mudstone), it can become a natural protective barrier of Cretaceous aquifer by changing coal mining technology or adjusting mining parameters, that is, it has the basic hydrogeological structure conditions for WPCM.

**Table 6** | Restriction of WCFZ height and mining height of No. 3 coal seam

Borehole	The distance between No. 3 coal and Cretaceous aquifer (m)	Restriction height of WCFZ (m)	Restriction of mining height (m)	Remark
K3-1	191.30	166.70	8.06	The thickness of safety water-resisting layer is 24.6 m.
K3-2	180.15	155.55	7.53	
K3-3	199.12	174.52	8.44	
K4-6	209.78	185.18	8.96	
K4-7	203.35	178.75	8.65	
K4-8	194.97	164.97	8.24	
G6-5	210.17	185.57	8.98	
G14-2	189.39	164.79	7.97	

### 3.2. Mining-induced overburden seepage laws

Permeability of mining rocks is an important parameter in engineering problems such as calculation of mine inflow and evaluation of water resistance of mining overburden during coal mining. In order to obtain the evolution laws of permeability of overlying strata in the study area during coal mining, the roof rock samples of Jurassic Yan'an Formation in Yonglong mining area, including fine sandstone and mudstone, were collected. An experimental study on the permeability of roof rock samples during the complete stress-strain path was carried out using the MTS electro-hydraulic servo experimental system. The experimental osmotic pressure difference was 1.5 MPa, the confining pressure was 5 MPa, and the pore pressure was 3.8 MPa. Figure 5 shows the complete stress-strain-permeability curve of rocks.

It can be seen from Figure 6 that the permeability coefficient of rocks gradually increased in the plastic deformation stage during the complete stress-strain process. When the axial stress reached the ultimate strength, the rocks were destroyed and interpenetrated by the formation of through fractures, and the permeability coefficient of rocks reached the maximum value. The permeability coefficient of medium sandstone varied from  $9.86 \times 10^{-7}$  to  $36.21 \times 10^{-7}$  cm/s, and the permeability coefficient of mudstone varied from  $3.67 \times 10^{-7}$  to  $10.25 \times 10^{-7}$  cm/s. These results suggested that the permeability of overlying rock of coal seam increases obviously under the influence of mining, and the maximum permeability coefficient of medium sandstone is 3.5 times that of mudstone. Combined with the research results of other scholars, the relationship between the average maximum permeability coefficient and the lithology of the overlying rocks in the complete stress-strain process is: mudstone < sandy mudstone < fine sandstone < medium and coarse sandstone (Wang & Park 2002; Meng *et al.* 2016). It can also be seen that after the permeability coefficient of overlying rocks reached the maximum value, the permeability coefficient decreased again, which indicated that within a period of time after mining, under the action of fractures closure and water expansion, the overlying rocks began to gradually recover its water-resisting ability. In particular, the mudstone in the overlying strata has a good self-recovery function after being damaged by mining, so that the damaged water-resisting layer can be reconstructed. Therefore, mudstone is the best water-resisting layer in water-preserved mining, and a high percentage of mudstone in the overlying strata is conducive to the implementation of water-preserved mining.

## 4. WATER-PRESERVED MINING TECHNOLOGIES IN THE STUDY AREA

Due to the large mining height of the No. 3 coal seam in Yonglong mining area and the limited thickness of rock layers between it and the Cretaceous aquifer, the WCFZ under the condition of fully mechanized caving mining can penetrate the Cretaceous aquifer, resulting in the loss of groundwater resources. Therefore, it is necessary to limit the height of WCFZ by changing the mining technologies and protect the stability of water-resisting key stratum, so as to achieve the dual purpose of roof water disaster prevention and groundwater resources protection.

### (1) Restriction of mining height

The average water column height of Cretaceous aquifer measured by 11 boreholes in the first mining panel of Cuimu coal mine in Yonglong mining area is 246.29 m. According to the regulation on water prevention and control in coal mines, the critical water inrush coefficient  $T_s$  of the complete aquiclude without fracture structure damage section is calculated as 0.1 MPa/m, and the thickness of safety water-resisting layer is 24.6 m. The

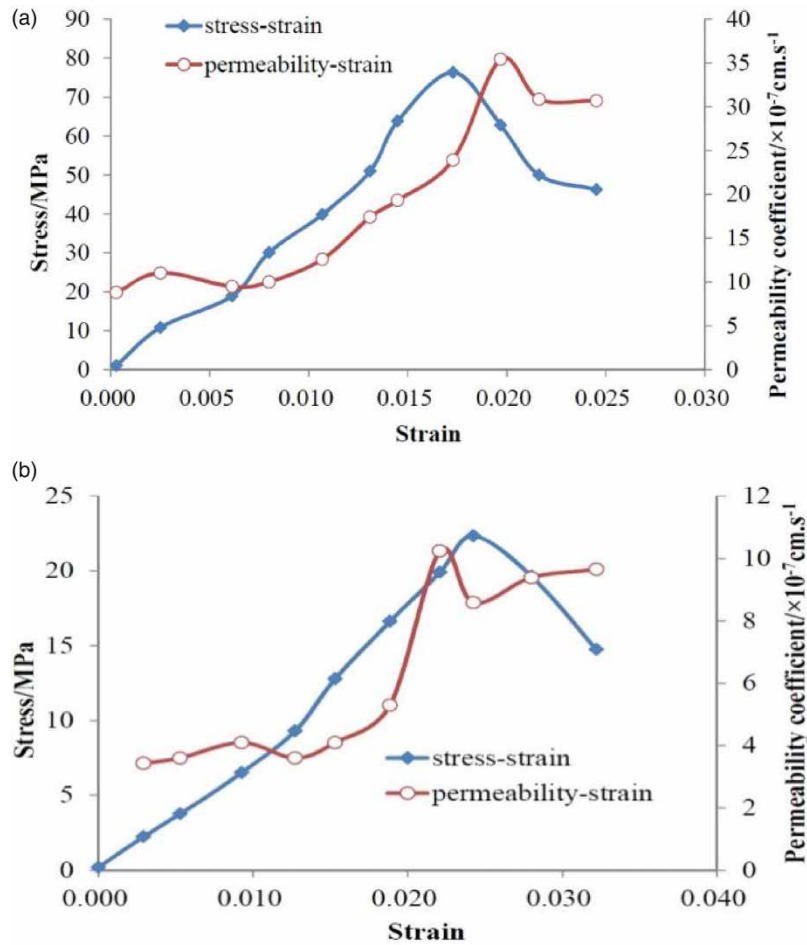


**Figure 5** | Complete stress–strain–permeability curves of overlying rocks above coal seam: (a) medium sandstone and (b) mudstone.

height of WCFZ is 20.67 times the mining height, and the restriction of mining height of each borehole can be calculated by the restricted height of WCFZ. The results show that when the mining height  $M \leq 9$  m, it can be ensured that the effective water-resisting layer thickness meets the requirement of the ultimate safety thickness of 24.6 m, and the WCFZ will not eventually reach the Cretaceous strata, which has no effect on the Cretaceous aquifer, as shown in Table 6.

## (2) Using the method of slice mining

The UDEC discrete element software was used to simulate and analyze the height of WCFZ in slice mining. The numerical model was established according to the stratigraphic configuration of G14-2 borehole. The mining conditions were as follows: near horizontal coal seam, the overlying strata of coal seam were homogeneous and medium hard, and the mining depth of No. 3 coal was 490 m. The single longwall caving mining method was adopted, and the roof was managed by all caving method. The average mining thickness of No. 3 coal was 11 m, and the mining was divided into two layers, the first layer was 3.5 m, and the second layer was 7.5 m.

The discrete element simulation results showed that during the excavation of the first layer of No. 3 coal, with the increase of the advance distance, the plastic zone area of the roof gradually increased, and the height also gradually increased. With the continuous increase of the advancing distance, the height of the plastic zone did not increase after reaching full mining, and the height of the plastic zone was basically stable. The height of WCFZ was determined to be 68 m according to the scope of the plastic zone (Figure 6(a)). During the excavation of the second layer of coal, with the increase of the advance distance, the plastic zone area of coal seam roof continued to expand upward on the basis of the plastic zone of the first layered mining, and its height gradually

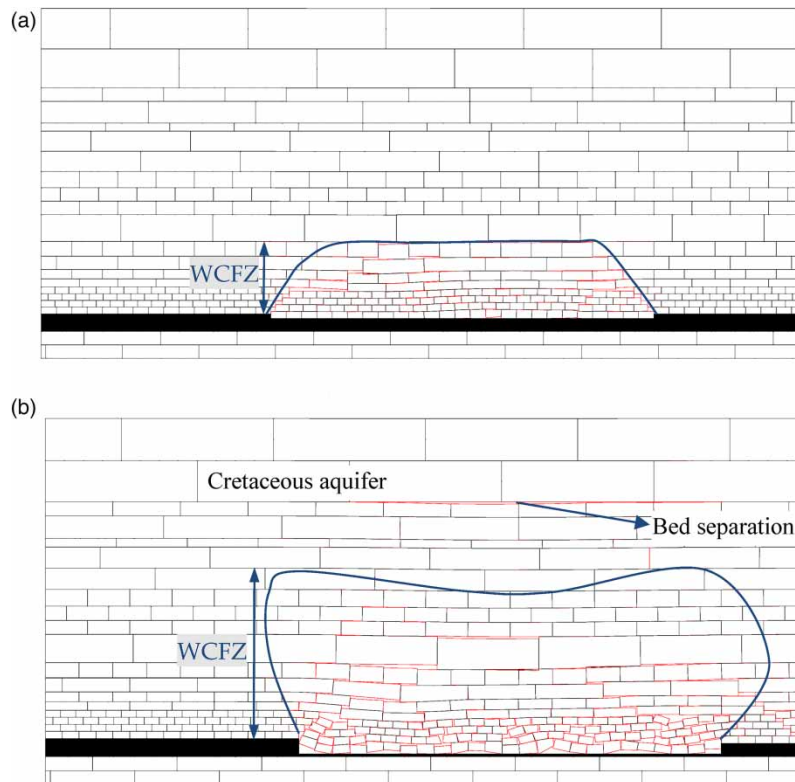


**Figure 6** | Fracture distribution in overlying strata after slicing mining of the No. 3 coal seam: (a) upper slicing mining and (b) lower slice mining.

increased. The height of plastic zone did not increase after the second layered mining reached full mining, and the height of the plastic zone was basically stable. According to the scope of the plastic zone and the fracture penetration, the height of WCFZ was determined to be 110 m (Figure 6(b)). The No. 3 coal of G14-2 borehole was 189.39 m from the Cretaceous strata, and the bottom interface of the Cretaceous strata was calculated to be 79.39 m from the WCFZ. It can be seen that the slice mining method can reduce the height of WCFZ so that it does not affect the Cretaceous aquifer, thus protecting the Cretaceous groundwater resources.

### (3) Controlling the advancing speed of working face

The contact zone between the glutenite at the bottom of Cretaceous strata and the mudstone of the Anding Formation at the top of the Jurassic strata is easy to form a bed separation space. A large amount of water is produced when groundwater infiltrates into the bed separation space. Its inrush not only threatens the safety of mine production, but also causes the leakage of Cretaceous groundwater resources (Li *et al.* 2018; Fan *et al.* 2019b).

According to the calculation formula of groundwater dynamics in confined aquifer, the calculation formula of unit width flow on the  $i$ th side of bed separation space is (Lyu *et al.* 2017):

$$q_i = k \cdot M \cdot \frac{\Delta H_i}{R_i} \quad (2)$$

where  $q_i$  is the unit width flow on the  $i$ th side of the separation space;  $k$  is the permeability coefficient of the aquifer within the bed separation range;  $M$  is the average thickness of the roof aquifer in the bed separation space;  $\Delta H_i$  is the water head difference between the aquifer and the bed separation space;  $R_i$  is the influence radius of the corresponding water level drawdown on the  $i$ th side of the separation space.

The formula for calculating the total amount of accumulated water in the separation space is:

$$Q_d = \sum_{i=1}^n q_i \cdot l_i \quad (3)$$

where  $Q_d$  is the total amount of accumulated water in the separation space;  $l_i$  is the length of the  $i$ th edge of bed separation space.

For example, the inclined length of No. 21302 working face of Cuimu coal mine is 202.5 m, and the mining height is 12 m. When the advancing distance of working face is 150 m, the relevant parameters are substituted into Equations (1) and (2) to calculate the volume of accumulated water under different mining speeds of working face, as illustrated in Figure 7. The results show that when the mining height is a constant, the volume of accumulated water is different under different mining speeds. The smaller the mining speed, the larger the accumulated water volume. When the mining height is 12 m and the mining speed is not more than 4 m/d, all the bed separation space is filled with water. When the mining speed is more than 4 m/d, the volume of unfilled water begins to appear in the separation space, and with the increase of mining speed, the amount of water accumulated in the separation space gradually decreases, and the volume of unfilled water in the separation space gradually increases. Considering the effect of mine pressure, it is suggested that the advancing speed of working face should be controlled at 6–7 m/d.

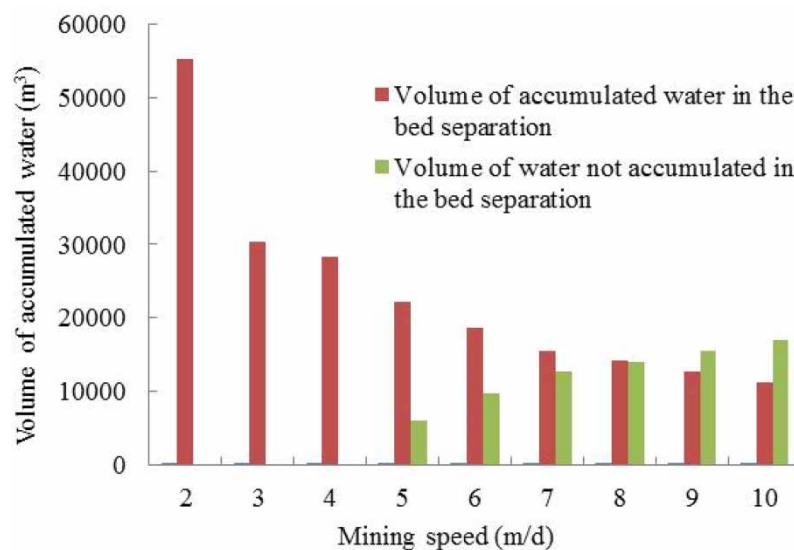


**Figure 7** | Relationship between advancing speed of working face and water accumulated volume in bed separation.

## 5. DISCUSSION

The applicability of WPCM technology is worth discussing. WPCM is proposed for the serious leakage of groundwater and the deterioration of ecological environment in the Salawusu Formation during the mining of Jurassic coalfields in northern Shaanxi, China. It is applicable to coal mines in the arid and semi-arid areas all over the world, and also has certain adaptability to the aquifer occurrence areas with ecological value. With the deepening of research, the scope of WPCM research is expanding, which is mainly due to the improvement of WPCM technology methods such as filling mining, slice mining, short-wall mining and grouting mining. Therefore, in the process of coal seam mining, as long as the aquifer or surface water body that needs to be protected is involved, the WPCM technology can be used to solve it. For example, the burnt rock water in the Shenfu mining area of China is one of the main groundwater resources. Coal mining experts have divided the water-preserved mining zone and put forward a new technology of burnt rock grouting curtain closure (Dong *et al.* 2019). The Office of Surface Mining, Reclamation and Enforcement (OSMRE) in the USA, assessed the impact of underground mining operations on streams and groundwater and proposed protective mining methods for water resources (Newman *et al.* 2017). The Neogene loose aquifer in the Balapukulia coal mine in Bangladesh not only threatens the mine safe production, but also has the significance of water supply. The feasibility of WPCM was discussed, and the mining mode of protecting the upper aquifer and dredging the lower aquifer based on water resources protection was proposed (Yu *et al.* 2019). Aquifer System in the Bogdanka Hard coal mine in the eastern part of Poland is of great ecological significance. The influence of mining on aquifer was analyzed, and the protection

technology of water-resisting key stratum was applied to avoid the mining-induced fracture channel from penetrating the overlying aquifer and realize water-preserved mining (Guzy & Malinowska 2020).

To conclude, WPCM provides an idea and way to release coal resources for water-coal symbiotic mines, but groundwater must be strictly treated as a resource. Active measures should be taken in the process of coal mining to protect water resources from waste and pollution. Although this technical specification is mainly proposed for the mining conditions of arid and semi-arid mining areas in western China, its extension is relatively wide, and it is feasible to carry out WPCM practice in mining areas where water resources need to be protected in countries around the world.

## 6. CONCLUSIONS

In order to protect the Cretaceous groundwater resources during the high-intensity mining in Yonglong mining area, China, this study investigated the hydrogeological structure and overburden engineering geological characteristics, analyzed the WCFZ height and mining fracture seepage laws, and proposed several WPCM technologies. The following conclusions were derived:

- (1) Yonglong mining area is rich in coal resources and poor in water resources, and the response of groundwater to coal mining is obvious. The main aquifer threatening the water filling and safety of No. 3 coal seam mining in the study area is the Cretaceous aquifer, which is not only an important water supply source in the region, but also the main source of water inrush, so WPCM should be implemented.
- (2) The development height of WCFZ in the Yonglong mining area was 17.1–23.5 times of the mining height, and the WCFZ in local area could penetrate the overlying Cretaceous aquifer. The mudstone aquiclude had strong expansion and disintegration, and the permeability coefficient was small after mining. Comprehensive geological conditions and mining-induced failure characteristics showed that the Yonglong mining area had the feasibility of carrying out WPCM.
- (3) Combined with the geological and mining conditions of the Yonglong mining area, the technical measures for WPCM were proposed, including limiting the mining height, adopting the slice mining method and reasonably selecting the advancing speed of the working face. These technologies effectively protected the Cretaceous groundwater resources.

## ACKNOWLEDGEMENTS

This research was supported by the Henan Province Scientific and Technological Plan Project (Grant Nos 232102320343 and 202102310218) and the Shaanxi Province Industrial Science and Technology Research Project (Grant No. 2016GY-172).

## DATA AVAILABILITY STATEMENT

Data cannot be made publicly available; readers should contact the corresponding author for details.

## CONFLICT OF INTEREST

The authors declare there is no conflict.

## REFERENCES

- Booth, C. J. 1986 Strata-movement concepts and the hydrogeological impact of underground coal mining. *Groundwater* **24**(4), 507–515.
- Booth, C. J. 2006 Groundwater as an environmental constraint of longwall coal mining. *Environ. Geol.* **49**, 796–803.
- Booth, C. J. & Bertsch, L. P. 1999 Groundwater geochemistry in shallow aquifers above longwall mines in Illinois, USA. *Hydrogeol. J.* **7**, 561–575.
- Cao, X. 2017 Policy and regulatory responses to coalmine closure and coal resources consolidation for sustainability in Shanxi, China. *J. Cleaner Prod.* **145**, 199–208.
- Dong, S. J., Yang, Z. B., Ji, Z. K., Wang, S. D., Gao, X. W. & Jiang, Q. 2019 Study on water - preserved mining technology of burnt rock aquifer beside the large reservoir in Shenfu mining area. *Int. J. Coal Sci. Technol.* **44**(3), 709–717.
- Fan, L. & Ma, X. 2018 A review on investigation of water-preserved coal mining in western China. *Int. J. Coal Sci. Technol.* **5**, 411–416.

- Fan, K., Li, W., Wang, Q., Liu, S., Xue, S., Xie, C. & Wang, Z. 2019a Formation mechanism and prediction method of water inrush from separated layers within coal seam mining: a case study in the Shilawusu mining area, China. *Eng. Fail. Anal.* **103**, 158–172.
- Fan, L., Ma, L., Yu, Y., Wang, S. & Xu, Y. 2019b Water-conserving mining influencing factors identification and weight determination in northwest China. *Int. J. Coal Sci. Technol.* **6**, 95–101.
- Gombert, P., Sracek, O., Koukouzas, N. & Gzyl, G. 2018 An overview of priority pollutants in selected coal mine discharges in Europe. *Mine Water Environ.* **38**, 16–23.
- Guo, W., Tan, Y., Bai, E. & Zhao, G. 2019 Sustainable development of resources and the environment: mining-Induced Eco-Geological environmental damage and mitigation measures – a case study in the Henan Coal Mining Area, China. *Sustainability* **11**, 4366.
- Guzy, A. & Malinowska, A. A. 2020 Assessment of the impact of the spatial extent of land subsidence and aquifer system drainage induced by underground mining. *Sustainability* **12**(19), 7871.
- Hickcox, D. H. 1980 Water rights, allocation, and conflicts in the Tongue River Basin, Southeastern Montana. *J. Am. Water Resour. Assoc.* **16**(5), 797–803.
- Li, H., Chen, Q., Shu, Z., Li, L. & Zhang, Y. 2018 On prevention and mechanism of bed separation water inrush for thick coal seams: a case study in China. *Environ. Earth Sci.* **77**, 1–12.
- Liu, J. & Elsworth, D. 1999 Evaluation of pore water pressure fluctuation around an advancing longwall face. *Adv. Water Resour.* **22**(6), 633–644.
- Lyu, G. L., Tian, G. J., Zhang, Y., Lyu, P. T., Chen, Y. B. & Shi, X. C. 2017 Division and practice of water-preserved mining in ultra-thick coal seam under ultra thick sandy conglomerate aquifer. *J. China Coal Soc.* **42**(1), 189–196.
- Meng, Z., Shi, X. & Li, G. 2016 Deformation, failure and permeability of coal-bearing strata during longwall mining. *Eng. Geol.* **208**, 69–80.
- Miao, X. X., Wang, A., Sun, Y. J., Wang, L. G. & Pu, H. 2009 Research on basic theory of mining with water resources protection and its application to arid and semi-arid mining areas. *China J. Rock. Mech. Eng.* **28**(2), 217–227.
- Newman, C., Agioutantis, Z. & Leon, G. B. J. 2017 Assessment of potential impacts to surface and subsurface water bodies due to longwall mining. *Int. J. Coal Sci. Technol.* **27**(1), 57–64.
- Qiu, H., Gui, H., Cui, L., Pan, Z. & Lu, B. 2019 Hydrogeochemical characteristics and water quality assessment of shallow groundwater: a case study from Linhuan coal-mining district in northern Anhui Province, China. *Water Supply* **19**(5), 1572–1578.
- Shi, X. & Zhang, J. 2021 Characteristics of overburden failure and fracture evolution in shallow buried working face with large mining height. *Sustainability* **13**(24), 13775.
- Sun, L., Chen, S. & Gui, H. 2016 Source identification of inrush water based on groundwater hydrochemistry and statistical analysis. *Water Pract. Technol.* **11**(2), 448–458.
- Thomas, J. L. & Anderson, R. L. 1976 Water-energy conflicts in Montana's Yellowstone River Basin, Southeastern Montana. *J. Am. Water. Resour. Assoc.* **12**(4), 829–842.
- Tiwari, A. K., Maio, M. D., Singh, P. K. & Singh, A. K. 2016 Hydrogeochemical characterization and groundwater quality assessment in a coal mining area, India. *Arabian. J. Geosci.* **9**, 1–17.
- Wang, J. A. & Park, H. D. 2002 Fluid permeability of sedimentary rocks in a complete stress-strain process. *Eng. Geol.* **63**(3), 291–300.
- Yu, Y. & Ma, L. 2019 Application of roadway backfill mining in water-conservation coal mining: a case study in Northern Shaanxi, China. *Sustainability* **11**(13), 3719.
- Yu, X. Y., Mao, X. W. & Guo, W. B. 2019 Coordinated waterproof mining mode under thick loose sand stratum in Barapukuria coal mine. *J. China Coal Soc.* **44**(3), 739–746.
- Zhang, J. 2005 Investigations of water inrushes from aquifers under coal seams. *Int. J. Rock Mech. Min. Sci.* **42**(3), 350–360.
- Zhang, D., Fan, G., Ma, L. & Wang, X. 2011 Aquifer protection during longwall mining of shallow coal seams: a case study in the Shendong Coalfield of China. *Int. J. Coal Geol.* **86**(2–3), 190–196.
- Zipper, C., Balfour, W., Roth, R. & Randolph, J. 1997 Domestic water supply impacts by underground coal mining in Virginia, USA. *Environ. Geol.* **29**, 84–93.

First received 6 May 2023; accepted in revised form 22 August 2023. Available online 31 August 2023